GEOPHYSICAL RESEARCH LETTERS, VOL. 20, NO. 20, PAGES 2187-2190, OCTOBER 22, 1993

EFFECTS OF STRONGLY TEMPERATURE-DEPENDENT VISCOSITY ON TIME-DEPENDENT, THREE-DIMENSIONAL MODELS OF MANTLE CONVECTION.

Paul J Tackley

Seismological Laboratory, California Institute of Technology

Abstract. Numerical simulations of thermal convection in a wide (8x8x1) Cartesian box heated from below with temperature-dependent viscosity contrasts of 1000, and Rayleigh number 10^5 show that boundary conditions and aspect ratio have an enormous effect on the preferred flow pattern. With rigid upper and lower boundaries, spoke-pattern flow with small (diameter ~ 1.5) cells is obtained, consistent with laboratory experiments and previous numerical results. However, with the arguably more realistic stress-free boundaries, the flow chooses the largest possible wavelength, forming a single square cell of aspect ratio 8, with one huge cylindrical downwelling surrounded by upwelling sheets. The addition of stress-dependence to the rheology weakens the stiff upper boundary layer, resulting in smaller cells, though still with upwelling sheets and downwelling plumes.

Introduction

Increasingly realistic numerical models of three-dimensional (3-D) thermal convection in planetary mantles have been published in recent years, with Rayleigh numbers approaching that of the Earth, and various other complexities such as spherical geometry, depth-dependent properties, and mineralogical phase changes [Bercovici et al., 1989; Balachandar et al., 1992; Tackley et al., 1993]. However, by far the largest approximation in these calculations is the assumption of viscosity which is constant, or only depth-dependent. The viscosity of the Earth's mantle is known to be very strongly temperature dependent, resulting in the formation of rigid surface plates, and strongly modulating the characteristics of other proposed features, such as plumes from the core-mantle boundary. Thus, it is essential to incorporate such rheology into numerical models.

Laboratory experiments have given some insights into variable viscosity convection, but are limited in their applicability to the Earth by the use of rigid boundary conditions, since the mobility ofplates on the Earth suggests that stress-free boundary conditions are appropriate. White [1988] determined that the spoke-pattern is prefered for rigid boundary conditions, Rayleigh numbers above about 25000 and large viscosity variations.

Numerical work has mainly focussed on steady-state solutions in small boxes. Ogawa et al. [1992] modeled viscosity contrasts of up to 10^5, identifying the stagnant lid regime, characterized by upwelling plumes and downwelling sheets beneath a stagnant lid, and the whole-mantle regime, characterized by up- and down-welling plumes with sheet-like extensions. Christensen and Harder [1991] determined that in small boxes (aspect ratio up to 1.5) temperature-dependent viscosity favors upwelling plumes and downwelling sheets. They also obtained a spoke-pattern solution for rigid boundary conditions in a 4x4x1 box with viscosity contrasts of 30. Perhaps the most prophetic result was obtained by Weinstein and Christensen [1991], who, in the same 4x4x1 box, found that simply changing the upper boundary condition to stress-free resulted in a much longer wavelength pattern consisting of upwelling sheets and a downwelling plume.

In order to understand the Earth's mantle, it is important to determine the flow patterns with stress-free boundaries at both top and bottom, with large viscosity contrasts, and in a box whose aspect ratio is similar to the effective aspect ratio of the Earth's mantle. Here, solutions with these characteristics are presented.

Model

In order to isolate the effect of variable viscosity, the Boussinesq approximation is assumed, with all coefficients constant except viscosity. The infinte Prandtl number equations, non-dimensionalized to thermal diffusion timescale (D^2/κ), mantle depth (D), and superadiabatic temperature drop (ΔT), are as follows:

$$\nabla\cdot\underline{v} = 0 \tag{1}$$

$$\nabla\cdot\underline{\underline{\tau}} - \nabla p = Ra_{1/2} T \underline{z} \tag{2}$$

$$\tau_{ij} = \eta(v_{i,j}+v_{j,i}) \tag{3}$$

$$\partial T/\partial t = \nabla^2 T - \nabla\cdot(\underline{v}T) \tag{4}$$

where $\underline{v}$, p, T, $\underline{\underline{\tau}}$, and η are velocity, dynamic pressure, temperature (varying from 0 at the top boundary to 1 at the base), deviatoric stress and dynamic viscosity, respectively, $\underline{z}$ is a unit vector in the vertical direction, and the Rayleigh number $Ra_{1/2}$ is defined using the viscosity at T=0.5 as follows:

$$Ra_{1/2} = \rho g \alpha \Delta T D^3/\eta_{1/2}\kappa \tag{5}$$

where ρ=density, g=gravitational acceleration, α=thermal expansivity and κ=thermal diffusivity. Viscosity is described by an Arrhenius law:

$$\eta_{New}(T) = \exp\,(13.8155(1/(T+1)-1/1.5)) \tag{6}$$

giving a variation between 100 and 0.1, with $\eta(0.5) = 1.0$

For the stress-dependence case:

$$\eta_{non\text{-}New} = \eta_{New}^{1/n}\, e^{1/n-1}\sigma_0^{1-1/n} \tag{7}$$

$$\eta_{eff} = 2\,(\eta_{New}^{-1} + \eta_{non\text{-}New}^{-1})^{-1} \tag{8}$$

where n is the power-law index, e is the strain rate and σ_0 is a reference stress. This gives Newtonian creep at low stresses, and non-Newtonian creep at high stresses.

Paper number 93GL02317
0094-8534/93/93GL-02317$03.00

The side boundaries are periodic, with top and bottom boundaries being isothermal (T=0 and 1 respectively) and impermeable, and either stress-free or rigid.

Numerical Method

The instantaneous velocity and pressure fields given by (1)-(3) are calculated by a finite difference (control volume) multigrid technique, using primitive variables ($\underline{v}$ and p) on a staggered grid [e.g., Patankar, 1980]. The iterative scheme is extremely robust, converging for almost any viscosity contrast. This scheme is incorporated into a standard multigrid V-cycle [Brandt, 1982; Press et al.,1992], giving convergence in order (number of points) operations. When stress-dependent viscosity is included, the viscosity field is re-calculated after every V-cycle. Explicit timestepping (equation (4)) is performed using the MPDATA algorithm [Smolarkiewicz, 1984] for advection, and second order finite-differences for diffusion. Steps of one-half the Courant condition are used. The method is well suited to parallel computers, and the presented results were obtained on the Intel Touchstone Delta at the California Institute of Technology.

Extensive benchmarking has been performed, in two dimensions against the standard benchmarks for constant [Travis et al., 1990] and temperature-dependent [Blankenbach et al., 1989] viscosity, and in three dimensions againt the results of Travis, Olson and Schubert [1990] for constant viscosity, and Ogawa et al. [1991] for viscosity contrasts of up to 3.2×10^4. For cases with Rayleigh number of order 10^5, agreement of the Nusselt number to 2% was found with 32 vertical grid cells.

Parameters

The four cases presented are listed in Table 1: one has constant viscosity, two have temperature-dependent viscosity and different boundary conditions, and one has stress-dependence added. All cases are entirely heated from below, with an aspect ratio of 8 in both horizontal directions, slightly less than the effective aspect ratio of the Earth's mantle (~10 at mid-depth), and 128x128x32 grid cells in the two horizontal and vertical directions respectively. $Ra_{1/2}$ is 10^5, two orders of magnitude lower than that of the Earth's mantle, but similar to that used in previous numerical and laboratory studies.

Cases were started from an identical initial state consisting of an isothermal interior (T=0.5), error-function boundary layers at top and bottom, and small random (white noise) perturbations of amplitude 0.05. After initial transients, the flow patterns were found to evolve very slowly but steadily, requiring large integration times (time≈0.2-0.4, 10000-19000 steps) to ensure solutions had overcome their transient nature and basal and surface Nusselt numbers were in good agreement.

In case 4, the nondimensional reference stress σ_0 was set to 500, approximately the mean stress from case 3, in order to weaken the upper boundary layer without getting the extreme viscosity variations obtained with non-Newtonian creep at all stress levels [Malevsky and Yuen, 1992].

Results

Temperature-dependent viscosity reduces the Nusselt number (Nu) and increases the mean temperature (T_{mean}), as listed in Table 1. The remainder of the discussion will focus on convective pattern.

The constant viscosity case (case 1) is illustrated in Figure 1a. There is a rough symmetry between up- and down-wellings, which both start off as sheets, decaying into plumes as they ascend or descend respectively. The downwellings exhibit greater connectivity in this very weakly time-dependent pattern, reflected in T_{mean} being slightly lower than 0.5; however, this is just by chance, since the equations are symmetric with respect to the vertical coordinate in this case. In small aspect-ratio boxes, stable patterns at this Rayleigh number include 2-D rolls, bimodal flow, and square or hexagonal cells, depending on the box dimensions and initial conditions [Travis et al., 1990]. The weakly time-dependent pattern obtained here lies somewhere between these idealized cases, also displaying some characteristics of the spoke pattern.

Case 2 (Figure 1b) has temperature-dependent viscosity and rigid boundary conditions. The spoke pattern is observed, as in laboratory experiments [White, 1988]. There is an asymmetry between up- and down-wellings, also noted by Christensen and Harder [1991]: downwelling sheets persist beyond mid-depth, whereas upwelling sheets have broken up into plumes by mid-depth.

A completely different pattern is obtained with stress-free boundary conditions (case 3, Figure 1c). Initially, many small cells formed, but over a nondimensional time of ~0.05 the downwellings merged to form one huge quasi-cylindrical downwelling, resulting in a single square cell filling the entire computational domain. Upwelling sheets extend all the way from the base to the surface. Although the overall pattern remained very stable throughout the remainder of the calculation, the exact details of upwellings and downwellings were highly time-dependent. Thus, two scales of flow were exhibited. In order to test the robustness of this solution to initial conditions, an additional calculation was done, starting from the final state of the rigid boundary case 2. After a nondimensional time of ~0.1, a single square cell was again formed. Stable long-wavelength flows resulting from temperature-dependent viscosity and stress-free boundaries have also been found in two-dimensional simulations [Davies, 1988a].

In case 4 (Figure 1d), the stress-dependent viscosity has resulted in softening of the stiff upper boundary layer, making it easier for it to enter the interior and hence resulting in smaller circulation cells. Again, upwelling sheets and downwelling plumes are obtained.

Discussion

The upwelling sheets and downwelling plumes found in the stress-free cases are compatible with the result obtained by Weinstein and Christensen [1991] in a 4x4x1 box with

TABLE 1. Simulation Characteristics

Case	Viscosity	Boundary Conds.	Time (steps)	Nu	Tmean
1	constant	stress-free	0.437(19600)	9.05	0.486
2	1000,n=1	rigid	0.353(14200)	4.15	0.674
3	1000,n=1	stress-free	0.188(10500)	6.22	0.629
4	1000,n=3	stress-free	0.231(15200)	8.91	0.602

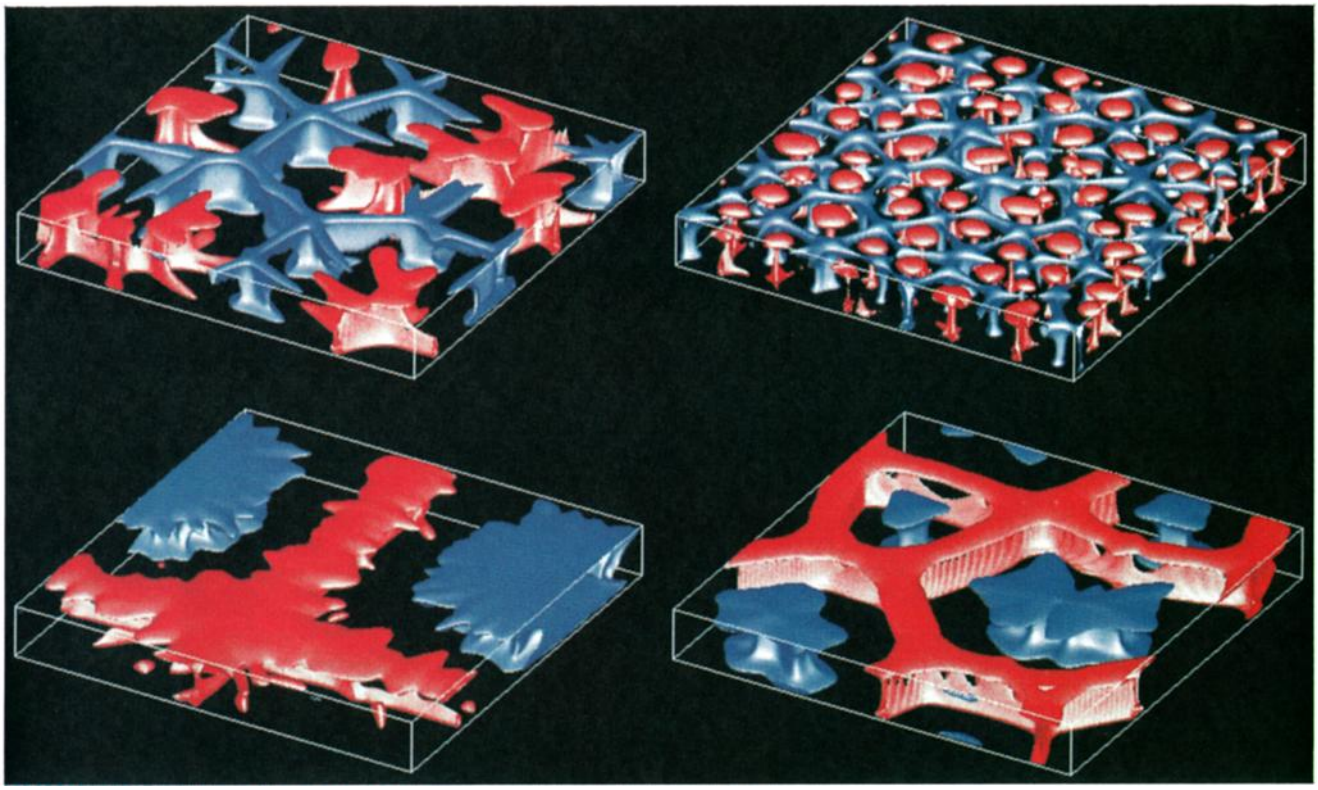

Fig. 1. Isocontours of residual temperature, showing where the temperature is higher (red) or lower (blue) than the horizontally-averaged value, by ±0.15 except where stated: a) (top left) Case 1, b) (top right) Case 2, c) (bottom left) Case 3, red contour is +0.1, d) (bottom right) Case 4, contours are ±0.1

isothermal, rigid lower and stress-free upper boundaries, and a viscosity contrast of 50. The pattern can be understood in the following terms: Depth-dependent properties cause the local Rayleigh number to decrease with depth, resulting in large cells with downwelling sheets and upwelling plumes [Balachandar et al., 1992]. In these simulations, the local Rayleigh number increases by 3 orders of magnitude with depth. Thus, the inverse flow pattern is obtained: upwelling sheets and downwelling plumes, with the viscous upper boundary layer imposing a long wavelength to the flow. Future calculations must establish the flow pattern when both depth-dependent properties and temperature-dependent viscosity are included, as well as the effects of spherical geometry, which favors upwelling plumes and downwelling sheets [Bercovici et al., 1989], and strong internal heating, which favors isolated cold plumes [Houseman, 1988]. If taken literally, the upwelling sheets would suggest active deep upwelling below mid-ocean ridges. However, this would seem to contradict various geophysical observables [Davies, 1988b]; thus the robustness of these features to the above mentioned effects must be tested.

Although linear slab-like downwellings are not obtained, on the Earth these occur almost exclusively at continental margins, suggesting that continents are necessary to obtain slabs. On Venus, the huge quasi-cylindrical downwellings may correspond to plateau-shaped highlands found in e.g., Ishtar Terra or Aphrodite Terra [Bindschadler et al., 1992].

In these simulations, the upper boundary layer participates in the flow. If the viscosity contrast were increased sufficiently, a 'stagnant lid' would develop [Ogawa et al., 1991], and the convective pattern might resemble the rigid boundary case, with small cells. However, the mobility of plates on the Earth suggest that this regime is not relevant to Earth dynamics, even though the viscosity contrast over the lithosphere may be extremely large. On Venus, the high surface temperature also raises doubts about the relevance of this regime.

Conclusions

These results show clearly the importance of stress-free boundary conditions and wide domains in understanding mantle convection with temperature-dependent viscosity. Very large cells are formed, with upwelling sheets and downwelling plumes, in contrast to the small-wavelength spoke pattern obtained with rigid boundary conditions. Although deep upwelling below mid-ocean ridges is suggested, the robustness of these patterns to internal heating, depth-dependent properties, spherical geometry and higher Rayleigh number needs to be established.

Acknowledgements: The author thanks David Stevenson, Slava Solomatov, Don Anderson and Marc Parmentier for useful discussions and suggestions, Gerald Schubert for a constructive review and Geoff Davies for alerting him to the potential of multigrid methods. The Intel Touchstone Delta system is operated by Caltech on behalf of the Concurrent Supercomputing Consortium. Access was provided by Caltech. Supported by NSF grant EAR9017893. Div. Geological and Planetary Sciences contribution number 5297.

References

Balachandar, S., D.A. Yuen and D. Reuteler, Time-dependent 3-dimensional compressible convection with depth-dependent properties, *Geophys. Res. Lett., 19*, 2247-2250, 1992.

Bercovici, D., G. Schubert and G.A. Glatzmaier, Three-dimensional spherical models of convection in the Earth's mantle, *Science, 244*, 893-1016, 1989.

Bindschadler, D. L., G. Schubert and W.M. Kaula, Coldspots and hotspots: Global tectonics and mantle dynamics of Venus, *J. Geophys. Res., 97*, 13495-13532, 1992.

Blankenbach, B., F. Busse, U. Christensen, L. Cserepes, D. Gunkel, U. Hansen, H. Harder, G. Jarvis, M. Koch, G. Marquart, D. Moore, P. Olson, H. Schmeleing and T. Scnaubelt, A benchmark comparison for mantle convection codes, *Geophys. J. Int., 98*, 23-28, 1989.

Brandt, A., Guide to multigrid development, in *Multigrid Methods: Proceedings Koln-Porz, 1981, Lecture Notes in Mathematics*, edited by Hackbusch W and U. Trottenberg, pp. 220-226, Springer-Verlag, Berlin, 1982.

Christensen, U. and H. Harder, 3-D convection with variable viscosity, *Geophys. J. Int., 104*, 213-226, 1991.

Davies, G.F., Role of the lithosphere in mantle convection, *J. Geophys. Res., 93*, 10451-10466, 1988a.

Davies, G.F., Ocean bathymetry and mantle convection 1. Large-scale flow and hotspots, *J. Geophys. Res., 93*, 10467-10480, 1988b.

Houseman, G., The dependence of convection planform on mode of heating, *Nature, 332*, 346-349, 1988.

Malevsky, A.V. and D.A. Yuen, Strongly chaotic non-Newtonian mantle convection, *Geophys. Astrophys. Fluid. Dyn., 65*, 149-171, 1992.

Ogawa, M., G. Schubert and A. Zebib, Numerical simulations of three-dimensional thermal convection in a fluid with strongly temperature-dependent viscosity, *J. Fluid Mech., 233*, 299-328, 1991.

Patankar, S.V., *Numerical Heat Transfer and Fluid Flow*, 197 pp., Hemisphere Pulishing Corporation, New York, 1980.

Press, W.H., S.A. Teulolsky, W.T. Vetterling, B.P. Flannery, *Numerical Recipes (Second Edition)*, 963 pp., Cambridge University Press, Cambridge, U.K., 1992.

Smolarkiewicz, P.K., A fully multidimensional positive definite advection transport algorithm with small implicit diffusion, *J. Comput. Phys., 54*, 325-362, 1984.

Tackley, P.J., D.J. Stevenson, G.A. Glatzmaier and G. Schubert, Effects of an endothermic phase transition at 670 km depth in a spherical model of convection in the Earth's mantle, *Nature, 361*, 699-704, 1993.

Travis, B.J., C. Anderson, J. Baumgardner, C.W. Gable, B.H.Hager, R.J. O'Connell, P. Olson, A. Raefsky and G. Schubert, A benchmark comparison of numerical methods for infinite Prandtl number thermal convection in two-dimensional Cartesian geometry, *Geophys. Astrophys. Fluid Dynamics, 55*, 137-160, 1990.

Travis, B.J., P. Olson and G. Schubert, The transition from two-dimensional to three-dimensional planforms in infinite-Prandtl-number thermal convection, *J. Fluid Mech., 216*, 71-91, 1990.

Weinstein, S.A. and U. Christensen, Convection planforms in a fluid with a temperature-dependent viscosity beneath a stress-free upper boundary, *Geophys. Res. Lett., 18*, 2035-2038, 1991.

White, D.B., The planforms and onset of convection with a temperature-dependent viscosity, *J. Fluid Mech., 191*, 247-286, 1988.

P.J. Tackley, Seismological Laboratory 252-21, California Institute of Technology, Pasadena, CA 91125.

(Received July 7, 1993;
Accepted August 13, 1993)